INTERNATIONAL ATOMIC ENERGY AGENCY
UNITED NATIONS EDUCATIONAL, SCIENTIFIC AND CULTURAL ORGANIZATION
INTERNATIONAL CENTRE FOR THEORETICAL PHYSICS
I.C.T.P., P.O. BOX 586, 34100 TRIESTE, ITALY, CABLE: CENTRATOM TRIESTE

SMR.703 - 15

WORKING PARTY ON
MECHANICAL PROPERTIES OF INTERFACES

23 AUGUST - 3 SEPTEMBER 1993

"Interfaces: Structure and Properties" (Part III)

"Effects of Atomic-Level Structural Disorder at Solid Interfaces: Elasticity and Melting"

Dieter WOLF
Materials Science Division
Argonne National Laboratory
9700 S. Cass. Avenue
Building 233
Argonne, IL 60439
U.S.A.

Effects of Atomic-Level Disorder at Solid Interfaces

Simon R. Phillpot, Dieter Wolf, and Sidney Yip

Introduction

The importance of interface materials is based largely on their inherent inhomogeneity, i.e., that the chemical composition and physical properties at or near an interface can differ dramatically from those of the nearby bulk material. For example, the propagation of a crack along an interface — rather than through the surrounding bulk material — indicates a different mechanical strength near the interface. Also, the elastic response and thermal behavior near an interface can be highly anisotropic in an otherwise isotropic material, and can differ by orders of magnitude from those of the adjacent bulk regions. Typically, these gradients extend over only a few atomic distances.

Because relatively few atoms control the properties in the interfacial region, the inherent difficulty in the experimental investigation of buried interfaces is actually an advantage in the atomic-level study of solid interfaces by means of computer-simulation techniques. While the limitations of such simulations are well known, this article will attempt to demonstrate the unique insights they can provide on some aspects of the mechanical behavior of both buried and thin-film interfaces. While to date, relatively little simulation work has focused directly on the observation of crack extension, we will discuss two types of phenomena with particular relevance in the fracture behavior of interface materials, namely their elastic and high-temperature properties. We will conclude with an outlook, too optimistic perhaps, on how the complementary capabilities of continuum-elastic theory, atomic-level computer simulation, and experiment could (and probably should) be combined in a new strategy for tackling the difficult problem of interface fracture to elucidate the underlying complex interplay between elasticity, plasticity, and temperature.

Structural Disorder at Interfaces

The most common form of structural disorder in a crystal lattice is caused by the thermal movements of the atoms or molecules, usually leading to thermal expansion. As is well known, this homogeneous type of disorder, and the consequent volume increase, originate in the anharmonicity of the interactions between the atoms. Due to the presence of planar defects, interface materials are structurally disordered even at zero temperature; however, because of its localization near the interface, this type of disorder is inhomogeneous. The effect on the volume is nevertheless similar, usually leading to a local volume expansion at the interface. In a way, volume expansion may thus be viewed as a measure of the amount of structural disorder in the system, both homogeneous and inhomogeneous. Another measure is the interface energy, which for grain boundaries (GBs) in metals has been shown to be directly related to the local expansion at the interface[1] (see also the article by Merkle and Wolf in the September 1990 *MRS BULLETIN*).

The radial distribution function, $r^2g(r)$, is a useful tool for characterizing the effects of structural disorder. As is well known, thermal disorder in an otherwise perfect crystal leads to two effects in $r^2g(r)$: First, the δ-function like zero-temperature peaks associated with the shells of nearest-, second-nearest, and more distant neighbors are broadened. Second, because of the volume expansion, the peak centers are shifted toward larger distances.

As illustrated in Figure 1, the structural disorder at a solid interface gives rise to the same two effects even at zero temperature. Figures 1a and 1b show the computed zero-temperature radial distribution functions, $r^2g(r)$, for atoms in the planes nearest- and next-nearest to a high-angle twist boundary on the (100) plane of an fcc metal.[1] While in the plane closest to the GB, the perfect-crystal δ-function peak structure (indicated by the arrows in Figure 1a) has been replaced by a broad distribution of interatomic distances, in the second closest plane, the ideal-crystal peaks have largely been recovered (see Figure 1b). This illustrates the highly localized nature of the structural disorder at the interface. Figure 1a also illustrates the cause for the expansion locally at the

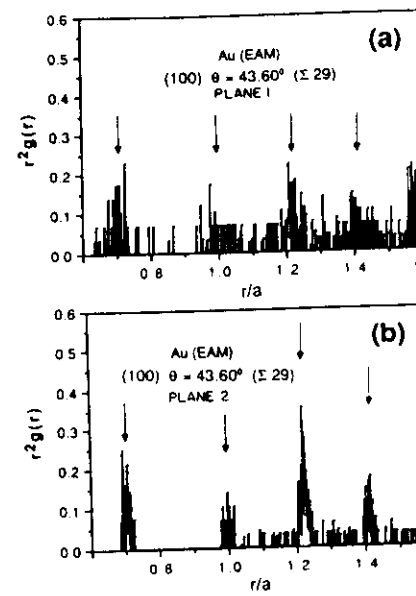

Figure 1. Radial distribution function, $r^2g(r)$, for the two planes nearest to a (100) θ=43.60° (Σ29) grain boundary as described by an EAM potential for Au. Arrows indicate the corresponding perfect-crystal peak positions. While atoms in the plane nearest to the interface (a) are very strongly affected by the presence of the interface, the atoms in the second-nearest plane (b) have an environment much closer to that of an ideal crystal.

GB. The distances to the left of the arrows represent atoms shoved more closely together than in the perfect crystal; because of the anharmonicity in the interatomic interactions, these atoms repel each other particularly strongly, resulting in a local expansion at the interface.

This article will illustrate two types of effects due to the local disorder at the interfaces, both alone and in combination with thermal disorder, particularly emphasizing their relevance to the mechanical behavior of interface materials. First, the investigation of the elastic behavior of model interface systems will provide an opportunity to study the interplay between the inhomogeneous effects of the local disorder at the interfaces and the homogeneous effects due to the resulting volume expansion. Then, the effect of thermal disorder on the high-temperature stability of a model grain boundary will be investigated, with particular focus on the possibility of "premelting" at the interface.

In both examples, the capability of simulations to probe a system in ways not experimentally possible will allow us to gain unique insights into the underlying causes. In investigating interface elasticity, the distinct effects of structural disorder and accompanying volume change can thus be separated. In the high-temperature study, by contrast, simulation demonstrates that there is no premelting and that every crystal can in principle melt by two distinct mechanisms, triggered by entirely different causes. While only one of the two types of melting is accessible experimentally, it is suggested that solid-state-amorphization experiments permit both types of "melting" to be investigated.

Elastic Properties of Interface Materials

The elastic response of materials is known to be particularly strongly affected by small changes in the volume, or in the underlying interatomic distances. For example, the thermal expansion of most materials, typically only a few percent between absolute zero and melting, causes an elastic softening, typically by about 50%. By comparison, the changes in interatomic distances due to the presence of interfaces may be considerably larger (see, for example, Figure 1), suggesting that the elastic response near an interface may differ dramatically from that of the nearby bulk perfect-crystal material. The supermodulus effect in composition-modulated strained-layer superlattices (see the article by Schuller et al. in this issue of the *MRS BULLETIN*) offers a glimpse of the different elastic moduli of interface materials, and of the opportunities for the engineering design of interface materials with mechanical properties unavailable in bulk materials.

Because the qualitative features of the structure and elastic properties of bulk interfaces, thin films and superlattices of fcc materials to be discussed have been found to be qualitatively identical whether described by a pair potential (Lennard-Jones) or an embedded-atom-method (EAM) potential,[2] results obtained using both types of potential will be used throughout.

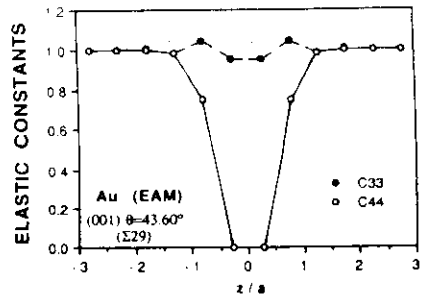

Figure 2. C_{33} and C_{44} (normalized to their bulk values) vs. distance from the (100) θ=43.60° (Σ29) grain boundary with radial distribution function shown in Figure 1. The z direction is parallel to the GB normal; hence C_{33} characterizes the effect of a strain in this direction, while C_{44} is associated with shear strains parallel to the GB. Each data point is averaged over the 29 atoms per (100) plane in the unit cell of the GB; the perfect-crystal spacing of (100) planes is 0.5a (where a is the lattice parameter). The grain boundary lies at z=0; the slight shift of the two planes next to the GB away from z=±0.25a is due to the volume expansion.

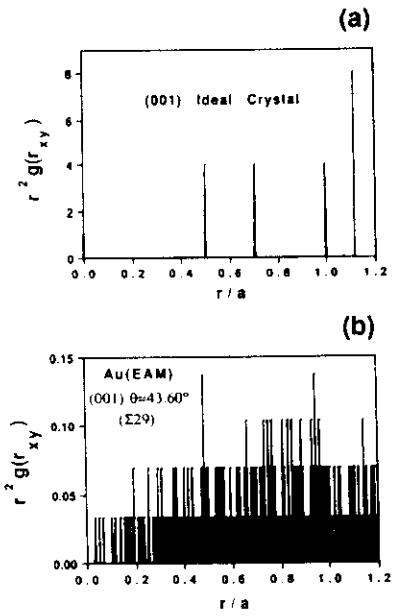

Figure 3. Pair correlation function, $r^2g(r_{xy})$, across (a) a perfect-crystal (100) plane and (b) the (100) θ=43.60° (Σ29) GB as described by an LJ potential parameterized to Cu. In the random-boundary model this distribution function characterizing the stacking of (100) planes across the GB is a constant, i.e., independent of r.

Local Elastic Constants at Grain Boundaries

Figure 2 shows the computed plane-by-plane elastic constants, C_{33} and C_{44}, for the atoms in the planes near the high-angle (100) twist boundary whose plane-by-plane radial distribution function is shown in Figure 1.[3] The important feature in this figure is the sharply contrasting behaviors of C_{33} and C_{44}: while C_{33} is essentially uniform through the GB (which is located at $z=0$), C_{44} decreases sharply at the interface, with a practically vanishing value in the two (100) planes immediately at the GB. Both behaviors can be understood in terms of the combined effects of the structural disorder at the GB and the consequent volume expansion.

We first consider the volume expansion at the GB, which one would expect to soften both elastic constants. For the shear constant, however, this volume expansion can only account for a decrease to approximately 60% of the bulk value.[3] The additional reduction in C_{44} must therefore be attributed to the presence of the GB.

To illustrate explicitly how the structural disorder at the GB leads to such a large softening in C_{44}, we analyze in detail the pair distribution function across the GB, $r^2g(r_{xy})$, shown in Figure 3. Here $r_{xy}=(x^2+y^2)^{1/2}$ is not the total separation between atoms as plotted in Figure 1 but rather the projection into the interface plane of the distance between atoms on opposite sides of the interface.[3] $r^2g(r_{xy})$ is therefore a measure of the quality of the stacking of (100) planes across the GB, i.e., of the degree of lateral interlocking of the atom positions across the interface. While $r^2g(r_{xy})$ in Figure 3a for an ideal crystal shows perfectly stacked (100) planes, the distribution in Figure 3b lacks almost any peak structure. The GB energy is therefore

modulated superlattice, however, A and B consist of the same material and are merely rotated with respect to each other about the interface normal by an angle θ (between A|B) and $-\theta$ (between B|A; see Figure 4). Figure 5a shows the elastic moduli of a series of GBSLs on the (100) plane of an fcc metal as a function of the modulation wavelength, Λ. According to Figure 5a an increase in the Young's and biaxial moduli in the z direction, Y_z and Y_{bz}, is coupled with a dramatic decrease in $G_{xz} \equiv C_{44}$. As can be seen from Figure 5b, this behavior in the elastic moduli is accompanied by an expansion in the z direction which, despite the resulting Poisson contraction in the (x-y) interface plane, gives rise to an overall expansion of the system which increases rapidly with decreasing Λ. Both the elastic and structural behavior of superlattices of grain boundaries thus mirror the basic properties of composition-modulated superlattices;[5] an in-depth analysis of the much simpler GBSLs thus promises to provide insights into the underlying causes for "supermodulus behavior."

A unique capability of simulation is that it permits the response of a system to be probed in ways often not possible experimentally. Four such studies have enabled elucidation of the distinct roles of the structural disorder at the interfaces, and the consequent dimensional changes, in the supermodulus effect.

First, the elastic constants of a GBSL were compared with those of a homogeneous perfect-crystal system with identical unit-cell dimensions but no interfaces.[6] It was found that volume expansion always leads to elastic softening, in accordance with our usual intuition gained from the study of homogeneous systems. However, as shown in Figure 6, C_{33} is dramatically strengthened relative to the homogeneous system, while C_{44} is further softened due to the presence of the interfaces in the GBSL.[6] The effects of the structural disorder can therefore be counter intuitive. It is interesting that, although C_{33} shows only a small overall enhancement over the related ideal-crystal value, Y_z (see Figure 5) is enhanced significantly. That these two results are not in conflict may be seen from the definition of the Young's modulus: $Y_z = C_{33} - 2C_{13}^2/(C_{11}+C_{12})$. Therefore, even though, with the exception of C_{33}, all elastic constants of the GBSL are actually softened with decreasing Λ, Y_z may be enhanced due to a complex interplay between various elastic constants associated with the in-plane response of the system. Thus the "supermodulus effect" may be aptly named, in that a "super elastic-constant" effect may not exist.

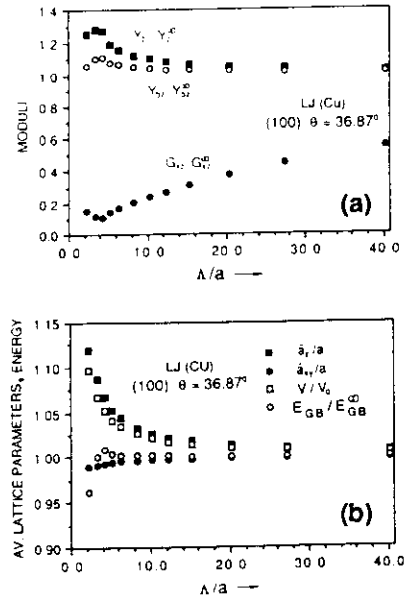

Figure 5. (a) Young's and biaxial moduli in the z direction (perpendicular to the interface planes) and modulus for shear parallel to the interfaces. (b) average lattice parameters, $\bar{a}_z$ and $\bar{a}_{xy}$, perpendicular and parallel to the interface planes, unit-cell volume normalized to the volume V_0 of a perfect-crystal reference system (i.e., without GBs). Also shown is the GB energy, E^{GB}; the superscript ∞ refers to the $\Lambda \to \infty$ (bulk) limit.

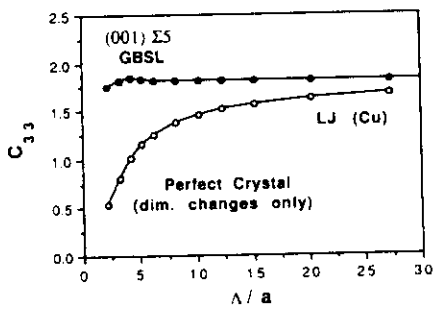

Figure 6. Elastic constant, C_{33}, in the direction of the interface normal (in 10^{12} dynes/cm^2) vs. Λ for the superlattice of (100) θ=36.87° (Σ5) grain boundaries (solid circles) and for a perfect reference system with the same orientation and unit-cell dimensions (open circles) as described by an LJ potential parameterized to Cu. These elastic constants describe the average response of the superlattice, by contrast with Figure 2 which shows the plane-by-plane local elastic constants of a buried interface.

Second, the extremes in the moduli Y_z, Y_{bz}, and G_{xz} in Figure 5a were shown to arise from the mutual attraction between the GBs in the superlattice, as evidenced by the rapid decrease in the GB energy for $\Lambda < 5a$ (see Figure 5b). This decrease signals a decreasing amount of structural disorder per interface as the elastic strain fields of different GBs start to overlap, with the consequence of smaller elastic anomalies.[7]

Third, by selectively suppressing the Poisson contraction in the interface planes, a manipulation not possible experimentally but straightforward in simulation, it was found that the Poisson effect always leads to increased disordering of the system and, hence, larger elastic anomalies.[4]

Finally, the above studies strongly suggest that the less inhomogeneous structural disorder there is in a system, the smaller the elastic anomalies should be. Since the GB energy is a direct measure of the amount of structural disorder in the system, one would expect the superlattices on a crystallographic plane with a lower GB energy should slow smaller elastic anomalies. The correctness of this intuition was verified by comparing the above results with superlattices of twist boundaries on the (111) plane, with a GB energy less than half that on the (100) plane[1,2] and, indeed, much smaller elastic anomalies and dimensional changes.[6]

Based on these insights gained from the study of GBSLs, one would expect that the two interfacial systems containing the least amounts of structural disorder, namely thin films (terminated by free surfaces) and *coherent* composition-modulated superlattices, should exhibit relatively small elastic anomalies. That this is indeed so is shown by Figure 7, which compares the shear constant, G_{xz} for GBSLs,[4] thin slabs[7], and coherent superlattices.[8] When structural disorder is reintroduced by removing the constraint of coherency at the interface, the elastic anomalies increase again toward their magnitudes in the GBSLs.[8]

Our investigation of the distinct roles played by the disorder localized at the interfaces and the accompanying volume changes has relied largely on the unique capability of computer simulation to explore relatively simple, well-characterized model systems in ways not usually possible experimentally. This approach permits the essential physics of the actual material to be exposed. We

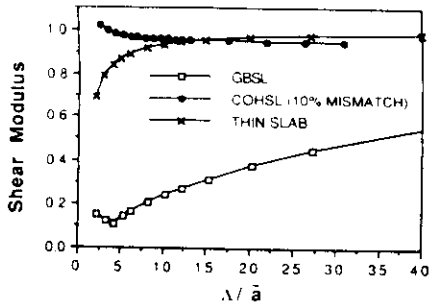

Figure 7. Shear modulus, G_m, normalized to the bulk ($\Lambda \to \infty$) value, as a function of Λ for a superlattice of (100) $\theta = 36.87°$ ($\Sigma 5$) grain boundaries (open squares) and for a thin slab of the same orientation (crosses) for a LJ potential parameterized to Cu. Also shown are data for a coherent (100) superlattice with a 20% misfit in the (LJ) lattice parameters (solid circles).

close by pointing out that although superlattices of grain boundaries may not be experimentally available, in several respects their properties should be closely related to those of single-material nanocomposites. As demonstrated in the article by R.W. Siegel in this issue of the *MRS BULLETIN*, the latter are also found to have some remarkable mechanical properties.

Role of Structural and Thermal Disorder in Melting

The ultimate process of thermal disordering in the solid state manifests itself in melting, where the material completely loses its long-range crystalline order. Despite its common occurrence and obvious importance in the study of materials properties, the atomic-level mechanism of melting is not well understood. Consequently, even less is known about the distinctions between high-temperature structural disordering processes in the bulk and at an interface. Clear experimental evidence, gathered from attempts to probe mechanisms of melting in various materials, points to the dominant effects of interfaces in the actual melting process.[9] In contrast, in several existing theoretical models of melting, the effects of surfaces, either internal or external, are generally not considered. In these theories melting is treated as a lattice instability associated with the atomic displacements exceeding a threshold value (Lindemann's criterion), with the vanishing of the shear modulus (Born's stability limit), or with the spontaneous generation of a critical concentration of vacancies.[10] By regarding melting as a homogeneous phenomenon, these models are unable to address the issue of melting at an interface, clearly an intrinsically heterogeneous process.

In terms of impact on mechanical properties, melting is probably the most significant of all phase changes because of the total loss of shear resistance. Given the experimental and theoretical difficulties of investigating structural disordering at an interface, it is not surprising that a fundamental understanding of how an interface affects the melting point of a material is still lacking. One can readily imagine that the presence of the interface simply alters the temperature at which the material melts as a whole. For example, based on Lindemann's criterion, one would expect a lower melting point near the interface, due to the larger vibrational amplitudes compared to the bulk crystal. But what is the mechanism involved? One can also imagine that the interface will have its own distinct melting point which, by virtue of the local structural disorder, may be expected to be lower than that of the bulk. This would then imply that a premelting transition exists where the interface becomes liquid at a temperature distinctly below the bulk melting point. The possibility of premelting at the GB, with attendant loss of local shear resistance, clearly would have very significant implications for the mechanical properties. Understandably, attempts have been made to look for premelting effects in GBs experimentally; as will be discussed below, simulation can contribute to the clarification of this basic issue.

Molecular dynamics (MD) simulations can contribute uniquely to the investigation of melting at interfaces, because they can address both its dynamic and thermodynamic (entropic) aspects at the atomic level. These simulations can provide insights not only into when melting should take place but also into why and how it occurs. The present illustration will use well-characterized bicrystal models to show that every crystal can, in principle, melt by two distinct physical causes. Thermodynamic melting, governed by the free energies of the crystalline and liquid phases, occurs by nucleation and growth of the liquid phase at interfaces, voids, or dislocations; it is therefore a *slow, heterogeneous* process. Mechanical melting, by contrast, is induced by an elastic instability causing the sudden collapse of the entire crystal lattice, and is therefore a *fast, homogeneous* process. It will be seen that the presence of the GB does not alter the bulk melting point; moreover, a premelting transition at the interface below the bulk melting point is not observed.

Molecular Dynamics Simulation of Thermodynamic Melting

We chose silicon as a model material to investigate the role of solid interfaces in the breakdown of crystalline order for several reasons. First, silicon has convenient crystal and liquid structures for distinguishing between crystalline and liquid-like local atomic environments. Second, an empirical interatomic potential function, constructed by Stillinger and Weber,[11] is available which permits a reasonably realistic overall description of the physical properties of silicon. For later reference, we note that a direct free-energy calculation yields a melting point, T_m, for this potential of 1691 K[12], which is close to the experimental value of 1683 K. Third, silicon is a good choice because extensive experimental data exist on its melting behavior, including the fact that it contracts upon melting. Finally, the mobility of GBs in pure silicon is known to be very low; any disordering arising from GB motion can thus be avoided, enabling a focus entirely on melting-induced structural disorder. To simulate a buried interface, the simulation cell is taken to be periodic in the two directions parallel to the GB plane, while in the direction of the GB normal, the simulation cell is surrounded on both sides by rigid perfect-crystal blocks which are allowed to slide parallel and perpendicular to the GB plane. This enables both GB migration and a volume expansion at the boundary.[13]

To monitor the local breakdown of long-range crystalline order during melting, we define an order parameter, $S(\mathbf{k})$, which characterizes the crystalline order within a given plane. $S(\mathbf{k})$ is defined as the square of the planar static structure factor, in which the wavevector $\mathbf{k}$ specifies the direction in which the ordering is being monitored.[14,15] $S(\mathbf{k})$ would have a value of 1 (0) if the atoms in the chosen plane are completely ordered (disordered). In a bicrystal, two order parameters, $S(\mathbf{k}_1)$ and $S(\mathbf{k}_2)$, are needed, one for each of the two semicrystals, thus enabling the identification of each plane as belonging to either of the two halves, or whether it is disordered altogether. In addition to planar ordering, it is also useful to monitor the local atomic environment of each atom through a coordination parameter C. In a perfect crystal

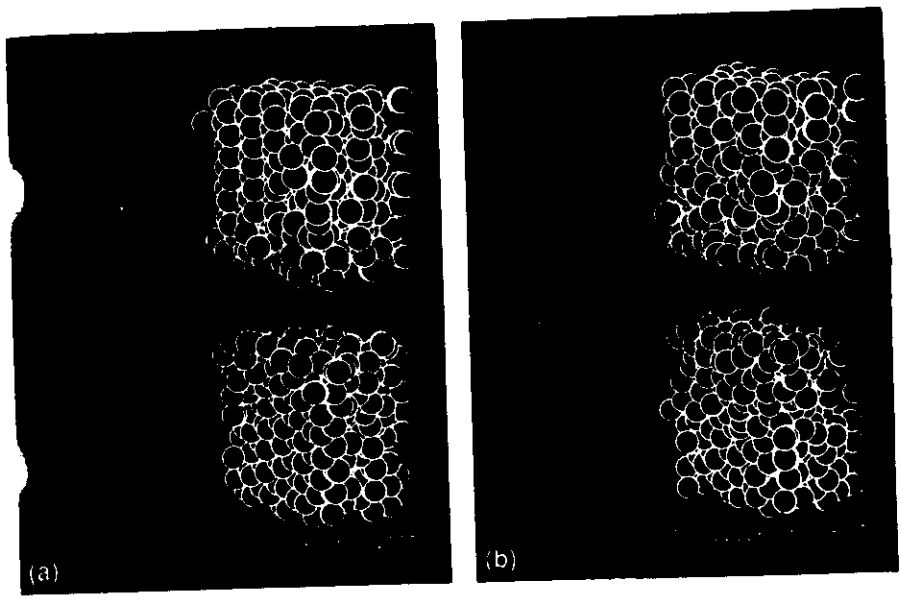

Figure 8. Heterogeneous "thermodynamic melting" of a silicon bicrystal containing in its center the (110) $\theta=50.48°$ ($\Sigma 11$) twist boundary. (The two semicrystals are pulled apart to facilitate visualization of the structural disorder.) After the bicrystal was heated from 1600 K ($T>T_m$) to 2200 K ($T>T_m$) over a period of 600 time steps (1000 steps corresponds to 1.15 picoseconds of real time), the simulation time was set to $t=0$. The shading of atoms indicates their nearest-neighbor coordination, C, with red, green and blue circles denoting, respectively, $C=4$, $C\geq 5$ and $C\leq 3$.
(a) After 2700 time steps, a number of planes on either side of the GB plane has melted. The near-zero values of the structure factors $S(k_1)$ and $S(k_2)$ how that long-range order has now broken down in approximately seven (110) planes closest to the GB. By contrast, at $t=0$ only a few atoms at the GB had coordination greater than four, and the structure-factor profiles showed a well-defined GB region consisting of about four (110) planes.
(b) After 8100 time steps, more than half the system has melted; long-range order has been lost in the 20 central planes of the system.

a silicon atom has four nearest neighbors ($C=4$), whereas in the liquid phase there are approximately six.

Figures 8a and 8b show two instantaneous atomic configurations in a bicrystal of silicon containing a (110) twist boundary; the simulation temperature of 2200 K is well above the melting point of the system T_m.[14,15] With the atoms colored according to their average nearest-neighbor coordination, C, it is clear that the interface region is highly disordered and that as the system evolves, the disordering is spreading into the bulk regions. On the left, the two related planar order parameters are shown; they too indicate that the (110) planes are disordered at the interface but well ordered in the bulk regions. To verify that the disordered region is indeed liquid (and not merely disordered, like an amorphous solid), the related volume contraction was determined and found to agree well with that extracted from an independent simulation of liquid silicon. Also, the mean-square displacement of the atoms in these planes increases linearly with simulation time; the value of the self-diffusion constant determined in this way also agrees well with that of the liquid at the same temperature.

The results of such simulations, carried out at several temperatures above T_m, allows the extraction of the velocity of propagation of the solid-liquid interfaces into the crystalline regions, v. The velocities are in good agreement with experimental values.[16] Figure 9 plots these velocities against temperature; extrapolation to zero velocity should yield an estimate of the coexistence temperature, T_m, at which the crystal and liquid are in thermodynamic equilibrium, and at which a solid-liquid interface therefore will not propagate. The temperature obtained this way from Figure 9 is 1710 ± 30 K, which is remarkably close to the value of $T_m=1691\pm 20$ K obtained from the free-energy analysis.

From this evidence, as well as from similar simulations for fcc metals,[17] it was concluded that above T_m the grain boundary nucleates the liquid phase which subsequently grows into the crystal, a process requiring thermally activated diffusion kinetics. The same conclusion was reached from a further investigation of the effects of extrinsic structural disorder on the dynamics of melting, via simulation of the effects at free surfaces[14,17] and voids.[17] The propagation velocities obtained for the solid-liquid interface nucleated at the (110) free surface of silicon are also shown in Figure 9.

Finally, the question of premelting at GBs can be addressed. An in-depth structural analysis of the interface at temperatures below T_m has found the (110) twist GB in silicon, on a plane with a large interplanar spacing, to be stable up to T_m.[14] The absence of any premelting effects was also observed in a more extensive study of a (100) twist boundary in Cu.[17] This is particularly interesting because the high mobility of the Cu GB observed in the simulations (by contrast with the immobile Si boundary) could easily be misinterpreted as disordering at temperatures below T_m. This conclusion agrees with recent electron microscopy measurements carried out specifically to investigate the possibility of a premelting transition.[18] Since earlier simulation studies had been interpreted as providing evidence for premelting, it may be useful to emphasize here the importance of the proper determination of T_m (via a free-energy calculation) and the use of proper border conditions in the simulation.[13,17]

Mechanical Melting

To induce melting in our simulations, it was necessary to superheat the crystal above T_m. The experimental difficulties in observing superheating are well known to be due to the inevitable presence of free surfaces and, in most materials, a sufficient atomic concentration of lattice dislocations.[19] In computer simulations, by contrast, extrinsic defects can be eliminated simply by using a perfect-crystal simulation cell with periodic border conditions in all three dimensions. Thermodynamic melting can thus be suppressed, allowing an investigation of how melting occurs in a homoge-

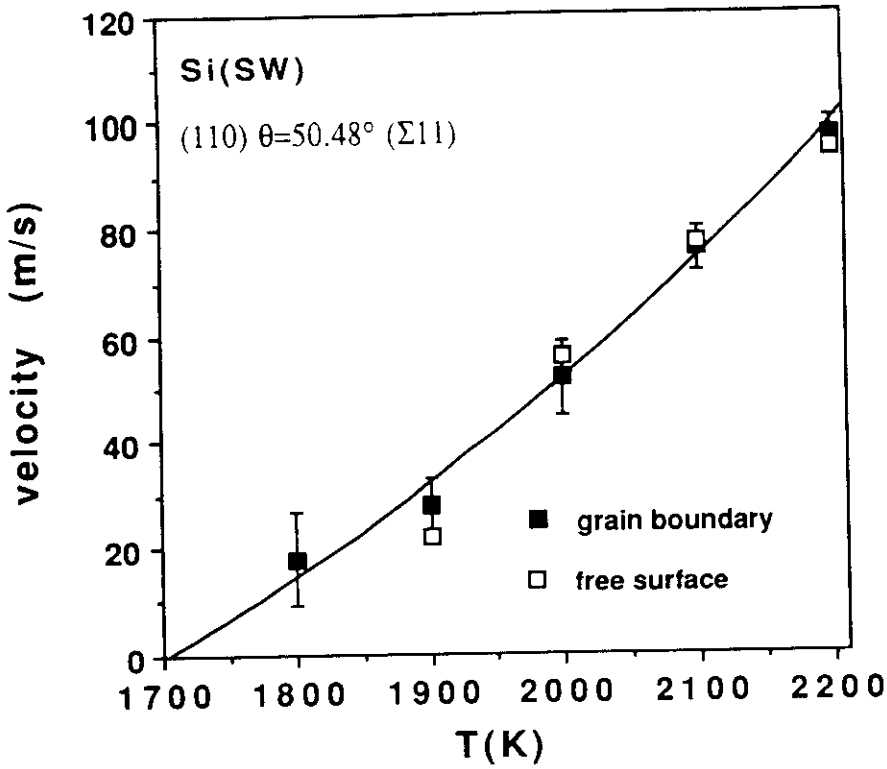

Figure 9. Propagation velocities of the solid-liquid interface as a function of temperature after nucleation from a grain boundary (solid squares with error bars) and from a free surface (open squares). The curve, representing a quadratic fit to the data points, extrapolates to zero velocity at $T=1710\pm30$ K.

neous system. From the viewpoint of structural disordering, this permits the distinct effects of homogeneous (i.e., thermal) and inhomogeneous disorder, due to the interfaces, to be separated.

Born has pointed out the existence of an ultimate stability limit for any crystal structure associated with the vanishing of the shear constant C_{44}.[10] For cubic crystals, and in the proper coordinate system, C_{44} is given by $(C_{11}-C_{12})/2$; this instability therefore occurs at a combination of temperature and volume where C_{11} and C_{12} become equal. Given that most materials expand upon heating, Born's criterion establishes a maximum superheating temperature, and a maximum volume expansion, above which the crystal is mechanically unstable and, therefore, has to undergo some kind of phase transformation (into the liquid state or into some other solid phase). The temperature associated with the maximum superheating limit under zero external pressure is referred to as the mechanical melting point, T_s, to be distinguished from the thermodynamic melting temperature, T_m. (The subscript "s" refers to stability.)[20]

Figure 10 illustrates a method for determining T_s from the elastic constants of a perfect fcc crystal which was superheated via MD simulation at constant pressure.[20] Extrapolation to the point where $C_{11}=C_{12}$ gives a value of T_s which is about 20% greater than T_m. (For Si, T_s is estimated to exceed T_m by as much as 40%; i.e., $T_s \approx 2500$ K.[12,14])

The mechanism of mechanical melting was investigated for both Si[15] and Cu[17] by simulating defect-free crystals at temperatures where the lattice should totally collapse. After a step increase of the simulation temperature to a value above T_s, only a few hundred MD time steps (equivalent to a few lattice-vibration periods) were required to completely destroy all long-range order. Moreover, the profiles of $S(\mathbf{k})$ showed that planar order was lost simultaneously in all parts of the crystal, suggesting that the liquid phase is formed *homogeneously*, as one would expect from an elastic or phonon instability.

Implications for Solid-State Amorphization

The simulations we have discussed demonstrate that every crystal can melt by two different processes—a "slow" heterogeneous process of nucleation and growth at an interface, and a "fast" homogeneous process triggered by a lattice instability. Since at ambient pressure, the volume expansion required for mechanical melting is always larger than that associated with thermodynamic melting, the free energy always favors thermodynamic over mechanical melting; i.e., $T_s>T_m$. However, as illustrated above, thermodynamic melting requires thermally activated atomic mobility and may therefore be kinetically hindered. The crystal then may not be able to disorder at the volume specified by equilibrium thermodynamics until a larger volume is reached at which the mechanical instability can occur.

There is considerable experimental evidence that solid-state amorphization, the process in which the long-range crystalline order is destroyed by external means (such as mechanical or chemical methods, or by irradiation), can proceed by the same two distinct mechanisms as melting. In contrast to a conventional melting experiment, however, both types of transition can actually be observed.[21] In a typical solid-state amorphization experiment, the temperature is held fixed at some relatively low value, well below T_m, while the volume is manipulated to increase toward the coexistence point in phase space where the thermodynamic transition should, in principle, occur. However, relatively low atom mobility can create a competition between the heterogeneous and homogeneous processes. Hence, while at higher temperatures mechanical amorphization will be preempted by the heterogeneous thermodynamics-based transition, at lower temperatures the latter may be kinetically hindered, and the homogeneous transition is observed.

Interface Fracture

The pronounced effects of structural and thermal disorder previously discussed can be expected to have a controlling influence on the mechanical properties of interfacial materials. However, the atomic-level understanding of intergranular embrittlement is a problem of even more formidable challenge to simulation, where now chemical disorder at the interfaces and plasticity

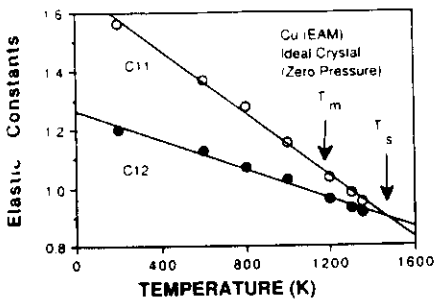

Figure 10. Calculated elastic constants C_{11} and C_{12} (in 10^{12} dynes/cm^2) vs. temperature for a perfect fcc crystal containing no extended defects which can therefore, in principle, be superheated to the maximum superheating limit, $T_s \sim 1432 \pm 12$ K. The solid lines are straight-line fits to the data points. An EAM potential fitted to Cu was used.

phenomena add new dimensions of complexity.

A simulation-based, integrated approach to the study of intergranular embrittlement should exploit the unique capabilities of a variety of simulation methods, outlined here for the case of GB fracture.[22] First, the GB energy (thought to play an important role in GB fracture) and its correlation with the underlying structure can be systematically investigated through lattice-statics simulations (see the article by Merkle and Wolf in the September 1990 issue of the *MRS BULLETIN*). Second, the dependence of the propensity for impurity segregation to the GB can be determined by Monte-Carlo simulation. While it has been recognized that the method of grand-canonical Monte-Carlo simulation should offer the most effective approach to the proper calculation of the distribution of solute segregants at the interface, only a few — albeit promising — results are yet available (see the article by Foiles and Seidman in the September 1990 issue of the *MRS BULLETIN*). Finally, the effect of external stress on the propagation of a crack, at or near a chemically equilibrated GB, can be directly observed by molecular dynamics.

It appears, however, that even such a comprehensive simulation-based approach, with the unique insights it can provide, represents only one of three building blocks required to better understand interface fracture. Clearly, the simulation results must be connected with experiments as well as incorporated into a continuum-elastic framework in order to understand the deformation and fracture behavior on a more macroscopic scale. As an example, to better understand crack-tip phenomena in brittle fracture, one could incorporate the local elastic constants obtained from atomistic simulations into elasticity equations for the stress analysis at a crack tip.[23] This combination of discrete-atom simulation with continuum theory and experiment could be further extended to a full study of intergranular fracture, where additional and highly localized interface effects, such as stress softening due to external loading (in a manner likely to be similar to thermal softening) and plastic deformation at the crack tip, could be systematically addressed through simulation. For example, a recent simulation study of the brittle-to-ductile transition in ideal-crystal fracture found that nonlinear and local effects of stress and temperature play an important combined role in the nucleation of dislocations at the crack tip.[24]

In conclusion, it is clear that despite the unique contributions simulations can make, only an approach using the complementary capabilities of atomistic simulation, macroscopic theory, and experiment holds promise in our quest to elucidate the intricate interplay between elasticity and plasticity, thermodynamics, and kinetics in the complex process of interface fracture.

Acknowledgments

This work was supported by U.S. Department of Energy BES-Materials Science under Contract No. W-31-109-Eng-38.

References

1. D. Wolf, *Acta Metall.* **37** (1989) p. 1983.
2. D. Wolf, J.F. Lutsko, and M. Kluge, in *Atomistic Simulation of Materials*, edited by V. Vitek and D.J. Srolovitz (Plenum Press, New York, 1989) p. 245.
3. M. Kluge, D. Wolf, J.F. Lutsko, and S.R. Phillpot, *J. Appl. Phys.* **67** (1990) p. 2370; D. Wolf and M. Kluge, *Scr. Metall.* **24** (1990) p. 907.
4. D. Wolf and J.F. Lutsko, *Phys. Rev. Lett.* **60** (1988) p. 12; *J. Mater. Res.* **4** (1989) p. 1427.
5. I.K. Schuller, *IEEE 1985 Ultrasonics Symposium*, edited by B.R. McAvoy (IEEE, New York, 1985) p. 1903; M. Grimsditch, in *Brillouin Scattering from Metallic Superlattices*, edited by M. Cardona and G. Guntherodt (Springer, Heidelberg, 1990).
6. D. Wolf, *Mater. Sci. Eng.* **A126** (1990) p. 1.
7. D. Wolf and J.F. Lutsko, *J. Appl. Phys.* **66** (1989) p. 1961; D. Wolf, *Acta-Scr. Met. Proc. Series* **4** (1990) p. 52; *Surf. Sci.* **225** (1990) p. 117.
8. S.R. Phillpot and D. Wolf, *Scr. Metall.* **24** (1990) p. 1109; J.A. Jaszczak, S.R. Phillpot, and D. Wolf, *J. Appl. Phys.* (in press).
9. R.W. Cahn, *Nature* **323** (1986) p. 668.
10. A.R. Ubbelohde, *The Molten State of Matter: Melting and Crystal Structure* (Wiley, Chichester, 1978); M. Born and K. Huang, *Dynamical Theory of Crystal Lattices* (Oxford, London, 1962).
11. F.H. Stillinger and T.A. Weber, *Phys. Rev. B* **31** (1985) p. 5262.
12. J.Q. Broughton and X.P. Li, *Phys. Rev. B* **35** (1987) p. 9120.
13. J.F. Lutsko, D. Wolf, S. Yip, S.R. Phillpot and T. Nguyen, *Phys. Rev. B* **38** (1988) p. 11,572.
14. S.R. Phillpot, J.F. Lutsko, D. Wolf, and S. Yip, *Phys. Rev. B* **40** (1989) p. 2831.
15. S.R. Phillpot, S. Yip, and D. Wolf, in *Computers in Physics* (Nov./Dec. 1990) p. 20.
16. M.D. Kluge and J.R. Ray, *Phys. Rev. B* **39** (1989) p. 1738; M.H. Grabow, G.H. Gilmer, and A.F. Bakker in *Molecular Dynamics Studies of Silicon Solidification and Melting*, (Mater. Res. Soc. Symp. Proc.) **141**, Pittsburgh, PA, 1989) p. 349.
17. J.F. Lutsko, D. Wolf, S.R. Phillpot, and S. Yip, *Phys. Rev. B* **40** (1989) p. 2841; J.F. Lutsko and D. Wolf, *Scr. Metall.* **22** (1988) p. 1923.
18. T.E. Hsieh and R.W. Balluffi, *Acta Metall.* **37** (1989) p. 1637.
19. J. Daeges, H. Gleiter, and J.H. Perepezko, *Phys. Lett. A* **119** (1986) p. 79.
20. D. Wolf, P.R. Okamoto, S. Yip, J.F. Lutsko, and M.D. Kluge, *J. Mater. Res.* **5** (1990) p. 286.
21. W.J. Meng, P.R. Okamoto, L.J. Thompson, B.J. Kestel, and L.E. Rehn, *Appl. Phys. Lett.* **53** (1988) p. 1820.
22. S. Yip and D. Wolf, *Mater. Sci. Forum* **46** (1989) p. 77.
23. F. Erdogan, *ASME J. Appl. Mech.* **52** (1985) p. 823.
24. K.S. Cheung, PhD thesis, MIT (1990), to be published. □

Equipment Exhibit at the 1990 MRS Fall Meeting...See p. 72